



This is a repository copy of *Temperature study of Al_{0.52}In_{0.48}P detector photon counting X-ray spectrometer*.

White Rose Research Online URL for this paper:
<http://eprints.whiterose.ac.uk/107003/>

Version: Accepted Version

Article:

Butera, S., Gohil, T., Lioliou, G. et al. (2 more authors) (2016) Temperature study of Al_{0.52}In_{0.48}P detector photon counting X-ray spectrometer. *Journal of Applied Physics*, 120 (17). 174503. ISSN 0021-8979

<https://doi.org/10.1063/1.4966940>

Reuse

Unless indicated otherwise, fulltext items are protected by copyright with all rights reserved. The copyright exception in section 29 of the Copyright, Designs and Patents Act 1988 allows the making of a single copy solely for the purpose of non-commercial research or private study within the limits of fair dealing. The publisher or other rights-holder may allow further reproduction and re-use of this version - refer to the White Rose Research Online record for this item. Where records identify the publisher as the copyright holder, users can verify any specific terms of use on the publisher's website.

Takedown

If you consider content in White Rose Research Online to be in breach of UK law, please notify us by emailing eprints@whiterose.ac.uk including the URL of the record and the reason for the withdrawal request.



eprints@whiterose.ac.uk
<https://eprints.whiterose.ac.uk/>

Temperature study of $\text{Al}_{0.52}\text{In}_{0.48}\text{P}$ detector photon counting X-ray spectrometer

S. Butera^{1a)}, T. Gohil¹, G. Lioliou¹, A. B. Krysa², A.M. Barnett¹

¹Semiconductor Materials and Device Laboratory, School of Engineering and Informatics, University of Sussex, Brighton, BN1 9QT, UK.

² EPSRC National Centre for III-V Technologies, University of Sheffield, Mappin Street, Sheffield, S1 3JD, UK.

A prototype 200 μm diameter $\text{Al}_{0.52}\text{In}_{0.48}\text{P}$ $\text{p}^+\text{-i-n}^+$ mesa photodiode (2 μm i-layer) was characterised at temperatures from 100 $^\circ\text{C}$ to -20 $^\circ\text{C}$ for the development of a temperature tolerant photon counting X-ray spectrometer. At each temperature, X-ray spectra were accumulated with the AlInP detector reverse biased at 0 V, 5 V, 10 V and 15 V and using different shaping times. The detector was illuminated by an ^{55}Fe radioisotope X-ray source. The best energy resolution, as quantified by the full width at half maximum (FWHM) at 5.9 keV, was observed at 15 V for all the temperatures studied; at 100 $^\circ\text{C}$ a FWHM of 1.57 keV was achieved, this value improved to 770 eV FWHM at -20 $^\circ\text{C}$. System noise analysis was also carried out and the different noise contributions were computed as functions of temperature. The results are the first demonstration of AlInP 's suitability for photon counting X-ray spectroscopy at temperatures other than ≈ 20 $^\circ\text{C}$.

I. INTRODUCTION

$\text{Al}_{0.52}\text{In}_{0.48}\text{P}$ is a III-V semiconductor that has recently started to receive attention for the development of photon counting X-ray spectrometers; at room temperature, non-avalanche [1] and avalanche photodiodes [2] have been shown to be sensitive to X-ray photons from ^{55}Fe radioisotope X-ray sources. Such systems have been shown to have energy resolutions of 930 eV and 682 eV, respectively, at room temperature [1, 2]. Due to its wide indirect bandgap (2.31 eV [3]), $\text{Al}_{0.52}\text{In}_{0.48}\text{P}$ is expected to be useful for building high-temperature tolerant X-ray spectrometers that can be beneficial in many applications including space missions and terrestrial applications

^{a)} Corresponding author. Electronic mail: S.Butera@sussex.ac.uk.

outside the laboratory environment. Furthermore, $\text{Al}_{0.52}\text{In}_{0.48}\text{P}$ is expected to have a reduced likelihood of damage from radiation and has been shown to present lower thermally-generated leakage currents than alternative narrow and wide bandgap materials (e.g. Silicon and AlGaAs) allowing operation at room temperature and above without cooling systems [4, 5], potentially this may result in cost savings due to reduced mass, volume and power requirements for such instruments. Because of its good linear attenuation coefficients as a consequence of the presence of Indium (atomic number 49), $\text{Al}_{0.52}\text{In}_{0.48}\text{P}$ has also higher X-ray quantum efficiency per unit thickness [1] compared to those of some other wide bandgap X-ray photodetectors, e.g. SiC, AlGaAs and GaAs [6, 7]. Moreover, it is nearly lattice matched with GaAs and the crystalline quality of the resultant material can be very high in comparison to III-V nitrides, IV and II-VI compounds of a similar bandgap. With respect to II-VI compounds, $\text{Al}_{0.52}\text{In}_{0.48}\text{P}$ also does not have disadvantages such as weakness of the crystalline lattice, which often results in high concentration of dislocation and native defects, and doping control problems in other materials [8].

All these properties make $\text{Al}_{0.52}\text{In}_{0.48}\text{P}$ a promising candidate material for the production of robust, compact and high-energy resolution X-ray spectrometers that can work over a broad range of temperatures.

X-ray photon counting spectroscopy at high temperatures has been previously reported using different wide bandgap semiconductor detectors made from materials such as SiC, $\text{Al}_{0.8}\text{Ga}_{0.2}\text{As}$, and GaAs. A SiC X-ray detector was demonstrated by Bertuccio et al. [9] with an energy resolution (FWHM) at 5.9 keV of 233 eV at 100 °C; whilst an $\text{Al}_{0.8}\text{Ga}_{0.2}\text{As}$ photodiode was reported by Barnett et al. [10] with energy resolution at 5.9 keV of 2.2 keV at 90 °C, limited by the noise of the preamplifier used. GaAs structures were also developed and characterised for use as X-ray spectrometers by Barnett et al. [11] and Lioliou et al. [12] with energy resolutions at 5.9 keV of 1.5 keV at 80 °C, and 840 eV at 60 °C, respectively. Other materials commonly considered for use at high temperatures for the detection of soft and hard X-rays, as well as γ -rays, include CdTe and its related compounds (e.g. CdZnTe, CdMnTe) [13]. At 92 °C, a FWHM at 122 keV of 53 keV was observed for CdTe [14]; whilst at 70 °C, a FWHM at 32 keV of 9.4 keV was reported for CdZnTe [15]. Despite their relatively poor energy resolutions, CdTe and CdZnTe are still attractive

choices for producing large area [16] and thick radiation detector, with adequate efficiency to high energy X- and γ -rays; spectroscopic CdZnTe and CdTe detector imaging arrays, for example, have also been demonstrated by Wilson et al. [17]. Good responses were also obtained for CdTe and CdZnTe under high X-ray photons flux [18, 19]. Abbene et al. [20] studied in detail the effects of energy, temperature and flux on the performance of a CdZnTe detector. Furthermore, recently work has been reported with CdZnTe detectors coupled to low noise application specific integrated circuit (ASIC) readout electronics, where a FWHM at 59.5 keV of 2.5 keV was demonstrated at room temperature [21].

In this paper a prototype non-avalanche (2 μm i-layer) 200 μm diameter $\text{Al}_{0.52}\text{In}_{0.48}\text{P}$ $\text{p}^+\text{-i-n}^+$ mesa photodiode was coupled to a custom-made low-noise charge-sensitive preamplifier of feedback resistorless design and characterised for its performance as a photon counting spectroscopic X-ray detector at temperatures from 100° C to -20 °C. The photodiode used was randomly selected from those produced as described in Section II; there was no pre-screening of photodiodes to select an optimally performing detector. System energy resolutions of 1.57 keV and 770 eV at 5.9 keV were observed at 100 °C and -20 °C, respectively. These significant results have been achieved because of the high performances of the $\text{Al}_{0.52}\text{In}_{0.48}\text{P}$ detector used and the custom charge-sensitive preamplifier electronics developed at our laboratory.

II. DEVICE STRUCTURE

The $\text{Al}_{0.52}\text{In}_{0.48}\text{P}$ wafer used in this work was grown using metalorganic vapour phase epitaxy (MOVPE). The $\text{Al}_{0.52}\text{In}_{0.48}\text{P}$ $\text{p}^+\text{-i-n}^+$ structure was grown lattice matched on a commercial (100) n-GaAs: Si substrate with a misorientation of 10 degrees towards $\langle 111 \rangle_A$ to suppress the CuPt-like ordered phase. The $\text{Al}_{0.52}\text{In}_{0.48}\text{P}$ n^+ -layer (0.1 μm thick) had a doping concentration of $2 \times 10^{18} \text{ cm}^{-3}$, it was doped using Si as n type dopant; the $\text{Al}_{0.52}\text{In}_{0.48}\text{P}$ p^+ -layer (0.2 μm thick) had a doping concentration of $5 \times 10^{17} \text{ cm}^{-3}$, it was doped using Zn as p type dopant. The $\text{Al}_{0.52}\text{In}_{0.48}\text{P}$ i-layer was 2 μm thick. A highly doped GaAs cap (10 nm thick) was grown on top of the $\text{Al}_{0.52}\text{In}_{0.48}\text{P}$ p^+ -layer to ensure good ohmic contact. Chemical wet-etched techniques were used to fabricate mesa diodes with diameter of 200 μm : the chemical etching process consisted in using 1:1:1 $\text{H}_3\text{PO}_4\text{:H}_2\text{O}_2\text{:H}_2\text{O}$ solution followed by 10 s in 1:8:80 $\text{H}_2\text{SO}_4\text{:H}_2\text{O}_2\text{:H}_2\text{O}$ solution. A Ti/Au (20 nm/200 nm) annular contact was deposited on top of the GaAs

layer of the structure to form the top ohmic contact; whilst a InGe/Au (20 nm/200 nm) contact was deposited onto the rear of the GaAs substrate to form the ohmic rear contact. The layer details of the $\text{Al}_{0.52}\text{In}_{0.48}\text{P}$ wafer are summarised in TABLE I.

TABLE I. Layer details of the $\text{Al}_{0.52}\text{In}_{0.48}\text{P}$ wafer.

Layer	Material	Thickness (μm)	Dopant	Dopant Type	Doping density (cm^{-3})
1	GaAs	0.01	Zn	p^+	1×10^{19}
2	$\text{Al}_{0.52}\text{In}_{0.48}\text{P}$	0.2	Zn	p^+	5×10^{17}
3	$\text{Al}_{0.52}\text{In}_{0.48}\text{P}$	2	Undoped		
4	$\text{Al}_{0.52}\text{In}_{0.48}\text{P}$	0.1	Si	n^+	2×10^{18}
5	Substrate n^+ GaAs				

III. EXPERIMENTAL RESULTS

A. Electrical characterisation

Leakage current measurements as a function of reverse bias were taken with the $\text{Al}_{0.52}\text{In}_{0.48}\text{P}$ photodiode reverse biased from 0 V to 15 V in 1 V increments and in dark conditions. A Keithley 6487 picoammeter/voltage source was used during the experiment; the uncertainty associated with the current readings was 0.3% of their values plus 400 fA, while the uncertainty associated with the applied biases was 0.1% of their values plus 1 mV [22]. The current across the $\text{Al}_{0.52}\text{In}_{0.48}\text{P}$ photodiode was studied in the temperature range 100 °C to -20 °C using a TAS Micro MT climatic cabinet to achieve and maintain the temperatures investigated. Figure 1 shows the current as a function of applied reverse bias at 100 °C. At temperatures below 80 °C, current values < 0.4 pA were measured.

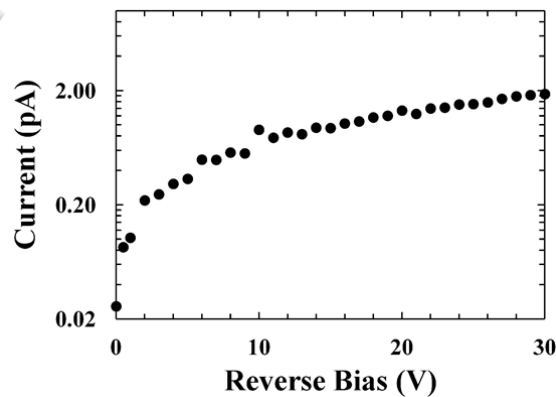


Figure 1. Dark current as a function of applied reverse bias at 100 °C for $\text{Al}_{0.52}\text{In}_{0.48}\text{P}$ device.

At a temperature of 100 °C, a dark current density $<0.6 \text{ nA/cm}^2$ was obtained for the $\text{Al}_{0.52}\text{In}_{0.48}\text{P}$ device when reverse biased at 15 V (75 kV/cm). This leakage current density was much smaller than has been reported with GaAs detectors at 100 °C (87 nA/cm^2) even when they were at lower electric fields (22 kV/cm) [12]. The measured leakage current density of the $\text{Al}_{0.52}\text{In}_{0.48}\text{P}$ (2 μm thickness) was comparable to the leakage current densities shown with high quality SiC (70 μm thickness) operated at 100 °C (1 nA/cm^2 at 103 kV/cm) [9].

Using an HP 4275A Multi Frequency LCR meter, the capacitance of the $\text{Al}_{0.52}\text{In}_{0.48}\text{P}$ packaged structure was measured as a function of applied reverse bias and temperature. The test signal was sinusoidal with a 50 mV rms magnitude and 1 MHz frequency. At each voltage and temperature, the capacitance of an identical empty package was also measured and subtracted from the measured capacitance of the packaged photodiode to determine the capacitance of the device itself. The uncertainty associated with each capacitance reading was $\pm 0.05 \text{ pF}$; the uncertainty associated with the applied biases was 0.1% of their values plus 1 mV. In the temperature range studied, the $\text{Al}_{0.52}\text{In}_{0.48}\text{P}$ capacitance was found to be $1.40 \text{ pF} \pm 0.05 \text{ pF}$, and voltage and temperature invariant within the limits of the measurement.

B. X-ray spectroscopy and noise analysis

The 200 μm diameter $\text{Al}_{0.52}\text{In}_{0.48}\text{P}$ photodiode was connected to a custom-made charge sensitive preamplifier of feedback resistorless design similar to that reported in ref. [23]. The output from the preamplifier was connected to an Ortec 572a shaping amplifier and then to a multichannel analyser (MCA). A 214 MBq ^{55}Fe radioisotope X-ray source ($\text{Mn K}\alpha = 5.9 \text{ keV}$, $\text{Mn K}\beta = 6.49 \text{ keV}$) was positioned 3 mm above the top of the $\text{Al}_{0.52}\text{In}_{0.48}\text{P}$ mesa photodiodes. X-ray spectra were collected at different applied reverse bias and temperatures. The $\text{Al}_{0.52}\text{In}_{0.48}\text{P}$ photodiode and the preamplifier were both placed inside the TAS Micro MT climatic cabinet for temperature control.

Spectra were accumulated with the diode reverse biased at 0 V, 5 V, 10 V and 15 V in the temperature range 100 °C to -20 °C. Although temperatures above 100 °C can be achieved by the TAS Micro MT climatic cabinet, temperatures higher than 100 ° were not studied because of limitations in the working temperature range of the

spectrometer electrical cables. The live time limit for each accumulated spectrum was 300 s. As the applied reverse bias was increased, an improvement in energy resolution (as quantified by the FWHM at 5.9 keV) was observed, this was due to improved charge collection at greater electric field strengths because the effects of reduced capacitance were negligible. The changes in the FWHM obtained at different shaping times (τ) were also studied; $\tau = 0.5 \mu\text{s}$, $1 \mu\text{s}$, $2 \mu\text{s}$, $3 \mu\text{s}$, $6 \mu\text{s}$, $10 \mu\text{s}$ were analysed. The ^{55}Fe photopeak obtained was the combination of the Mn $K\alpha$ and Mn $K\beta$ lines at 5.9 keV and 6.49 keV, respectively. Gaussians were fitted to the peak taking into account the relative X-ray emission rates of the ^{55}Fe radioisotope X-ray source at 5.9 keV and 6.49 keV in the appropriate ratio [24] and the relative difference in efficiency of the detector at these X-ray energies. Figure 2 shows the best energy resolution (smallest FWHM) spectra at 100°C (a), at 20°C (b), and at -20°C (c), when the diode was reversed bias at 15 V.

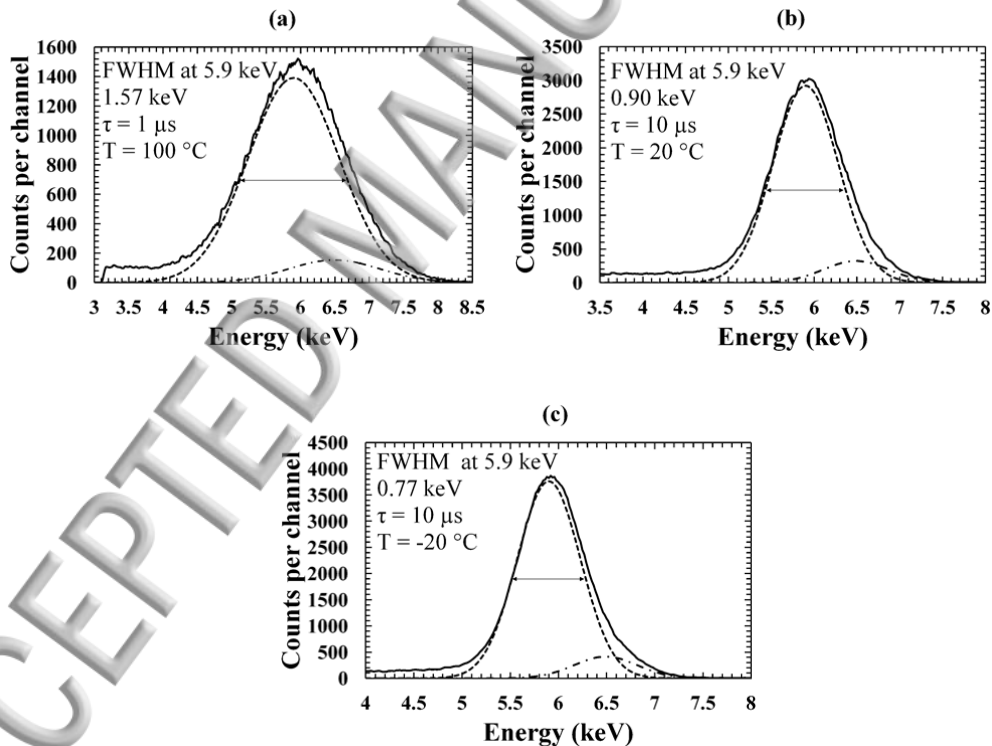


Figure 2. ^{55}Fe X-ray spectrum accumulated at 15 V reverse bias using the $\text{Al}_{0.52}\text{In}_{0.48}\text{P}$ device at a) 100°C , b) 20°C , and c) -20°C . Also shown, in each spectrum, are the fitted Mn $K\alpha$ (dashed line) and Mn $K\beta$ (dashed-dot line) peaks.

As shown in Figure 2, energy resolutions (FWHM) at 5.9 keV of 1.57 keV and 770 eV were obtained at 100°C and at -20°C , respectively. The FWHM at 5.9 keV at 20°C was 900 eV.

The FWHM was measured for all the spectra accumulated. Figure 3 shows the FWHM of the 5.9 keV peak as a function of temperature for the shaping time in the 0.5-10 μ s range at which minimum FWHM was found, when the $\text{Al}_{0.52}\text{In}_{0.48}\text{P}$ device was reversed bias at 15 V.

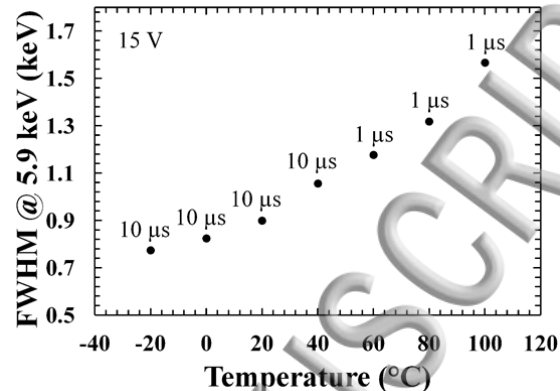


Figure. 3 FWHM of the 5.9 keV peak as a function of temperature at the optimum shaping time and at 15 V.

An increased FWHM was observed at increased temperatures; this was in part attributed to the higher contribution of the parallel white noise of the system as the temperature increased.

Three different classes of noise degrade the energy resolution (FWHM) of non-avalanche X-ray photodiode spectrometers. These are the Fano noise, the charge trapping noise, and the electronic noise [25]. The statistical nature of the charge creation process at the absorption of an X-ray determines the Fano noise; the expected Fano limited resolution at 5.9 keV for $\text{Al}_{0.52}\text{In}_{0.48}\text{P}$ at room temperature was calculated to be 145 eV, considering an electron-hole pair creation energy of 5.34 eV [26] and assuming a Fano factor of 0.12. The FWHM at 5.9 keV experimentally observed at 20 °C was greater than the Fano limited resolution, this highlighted that there was a significant contribution from at least one of the other noise sources. The electronic noise, due to the $\text{Al}_{0.52}\text{In}_{0.48}\text{P}$ photodiode and the preamplifier, consists of parallel white noise, series white noise, induced gate current noise, $1/f$ noise and dielectric noise [25, 27, 28]. The parallel white noise takes into account the leakage currents of the detector and input JFET of the preamplifier, it is directly proportional to the shaping time. The series white noise takes into account the capacitances of the detector and input JFET of the preamplifier, it is inversely proportional to the shaping

time. The series white noise power spectral density can be approximated to the thermal noise of the JFET drain current when stray resistance in series with the JFET gate is negligible. The series white noise was calculated using the capacitance and was adjusted for induced gate current noise [25, 27]. $1/f$ noise is instead independent from the shaping time. Figure 4 shows the computed parallel white noise, series white noise, $1/f$ noise at shaping times of 1 μ s and 10 μ s, respectively, when the $\text{Al}_{0.52}\text{In}_{0.48}\text{P}$ detector was reversed bias at 15 V.

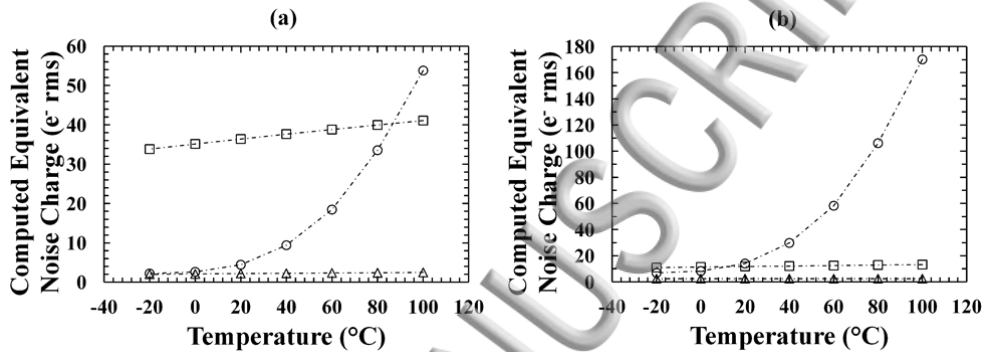


Figure 4. Computed equivalent noise charge as a function of temperature using the $\text{Al}_{0.52}\text{In}_{0.48}\text{P}$ device at shaping times of a) 1 μ s and b) 10 μ s. In both graphs the parallel white noise (empty circles), the series white noise (empty squares) and the $1/f$ noise (empty triangles) contributions are shown; interpolating lines between the experimental data points (dashed-dot lines) are also shown but must be considered guides for the eye only.

The combined contribution of the dielectric noise and charge trapping noise at 5.9 keV was calculated by subtracting in quadrature the Fano noise, parallel white noise, series white noise, and $1/f$ noise contributions at 5.9 keV from the measured FWHM at 5.9 keV. Figure 5 shows the calculated combined dielectric and trapping noise contributions at 5.9 keV as a function of temperature, when the $\text{Al}_{0.52}\text{In}_{0.48}\text{P}$ photodiode was reversed bias at 15 V.

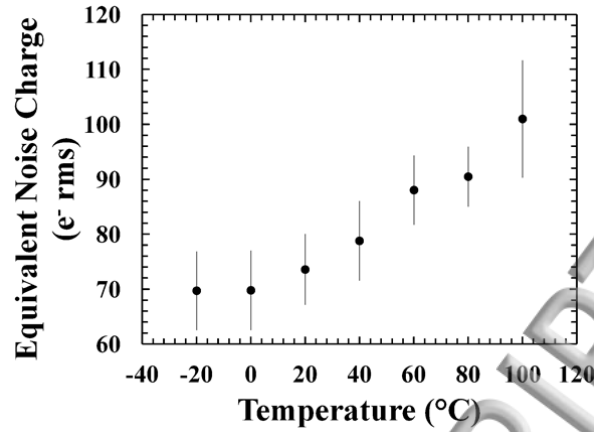


Figure. 5. Equivalent noise charge of the dielectric and trapping noise contribution at 5.9 keV as a function temperature.

The dielectric and trapping noise contribution at 5.9 keV increased from (70 ± 7) eV to (101 ± 10) eV, when the temperature was increased from -20 °C to 100 °C. At 15 V, the charge trapping noise was negligible as a consequence of improved charge transport at higher electric fields, in accordance with ref. [1]. Therefore, the increase in the equivalent noise charge, observed in Figure 5, can be attributed to the dielectric noise contribution increasing when the temperature was increased. The dependence of the dielectric equivalent noise charge (ENC_D) from the temperature is given by,

$$ENC_D = \frac{1}{q} \sqrt{A_2 2kTDC} \quad (1)$$

where q is the electric charge, A_2 is a constant (1.18) depending on the type of signal shaping [27], k is the Boltzmann constant, D is the dissipation factor and C is the capacitance [25]. A linear least squares fit of the square of the dielectric noise data showed a linear dependence on the temperature. The gradient determined by the linear least squares fit was $(45 \pm 6) [e^- \text{ rms}]^2 K^{-1}$; an effective dielectric dissipation factor as high as $(7.0 \pm 0.9) \times 10^{-3}$ was estimated, but it should be noted that this does not correspond directly to the dissipation factor of $Al_{0.52}In_{0.48}P$, rather it is indicative of the effective combined dissipation factor of all dielectrics contributing to this noise as it is analyzed here. Figure 6 shows the corresponding linear least squares fit. Comparison of the standard deviations of the fitting with the experimental uncertainties demonstrated that linear fitting was appropriate within the limitations of the experiment.

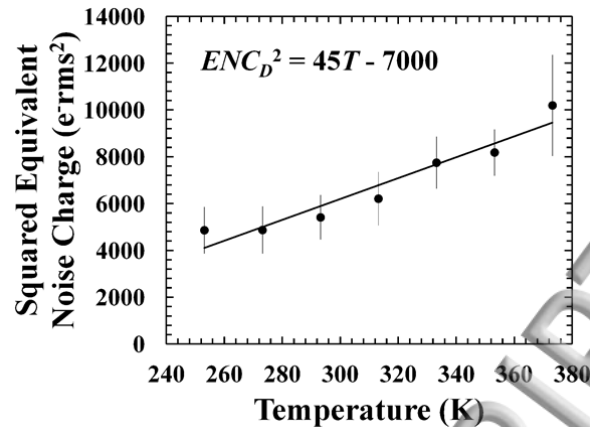


Figure. 6. Squared equivalent noise charge (ENC_D^2) of the dielectric noise at 5.9 keV as a function temperature in Kelvin (circles). Also shown is the line of the best fit computed by linear least squares fitting.

The energy resolutions at 5.9 keV for the $Al_{0.52}In_{0.48}P$ photodiode at high temperatures were worse than the energy resolutions at 5.9 keV observed for SiC and GaAs detectors at the same temperatures. At 100 °C, a FWHM of 1.57 keV at 5.9 keV was obtained here, whilst a FWHM of 233 eV at 5.9 keV was reported by Bertuccio et al. [9] for SiC detectors. The better energy resolution observed by Bertuccio et al. [9] was attributed to the lower electronic noise associated with their device' readout electronics, the thicker detector (lower capacitance) and also the extremely high quality materials used. At 60 °C, a FWHM of 1.12 keV at 5.9 keV was achieved here, whilst a FWHM of 840 eV at 5.9 keV was obtained by Lioliou et al. [12] for GaAs detectors. Since in the presently reported $Al_{0.52}In_{0.48}P$ study device readout electronics similar to Lioliou et al. [12] was used, the better performance of the GaAs X-ray spectrometer was in part attributed to the lower electron hole pair creation energy of GaAs [29] with respect to that one of $Al_{0.52}In_{0.48}P$. For example, a total noise at the input of the preamplifier of 86 e⁻ rms corresponds to 840 eV in GaAs, whilst the same noise equates to a resolution of 1.08 keV in $Al_{0.52}In_{0.48}P$, due to the difference in electron-hole pair creation energy. The FWHM observed at 5.9 keV for the $Al_{0.52}In_{0.48}P$ spectrometer was greater than 1.08 keV suggesting a slightly higher total noise for the $Al_{0.52}In_{0.48}P$ spectrometer (93 e⁻ rms) with respect to the previously reported GaAs spectrometer (86 e⁻ rms) [12]. The 93 e⁻ rms total noise in the $Al_{0.52}In_{0.48}P$ system was calculated by summing in quadrature the 12 e⁻ rms Fano noise (c.f. 13 e⁻ rms in GaAs [12]), the 58 e⁻ rms parallel white noise (c.f. 43 e⁻ rms in GaAs [12]), the 13 e⁻ rms series white noise (c.f. 25 e⁻ rms in GaAs [12]), the 2.5 e⁻

rms $1/f$ noise (c.f. $4.6 e^-$ rms in GaAs [12]) and the $83 e^-$ rms dielectric noise (c.f. $70 e^-$ rms in GaAs [12]). The energy resolution achieved with the $Al_{0.52}In_{0.48}P$ detector was, instead, better than that reported by Barnett et al. using $Al_{0.8}Ga_{0.2}As$ detectors [10]. At $90^\circ C$, a FWHM of $2.2 keV$ at $5.9 keV$ was obtained by Barnett et al. [10], although the readout electronics used in Ref. 10 were not of identical design as those used here.

III. CONCLUSION

In this paper, a non-avalanche $200 \mu m$ diameter $Al_{0.52}In_{0.48}P$ p^+-i-n^+ mesa X-ray photodiode was coupled to a custom-made charge-sensitive preamplifier for the development of a high temperature tolerant X-ray spectrometer. The detector was illuminated with an ^{55}Fe radioisotope X-ray source. The system was characterised over the temperature range $100^\circ C$ to $-20^\circ C$. A dark current density $\leq 0.6 nA/cm^2$ at $100^\circ C$ was obtained for the $Al_{0.52}In_{0.48}P$ device at $15 V$ ($75 kV/cm$). X-ray spectra were accumulated with the diode reverse biased at $0 V$, $5 V$, $10 V$, and $15 V$, as a function of temperature; the best energy resolution (as quantified by the FWHM at $5.9 keV$) was observed at $15 V$. At $100^\circ C$, the best energy resolution was $1.57 keV$ (FWHM at $5.9 keV$) using a shaping time of $1 \mu s$; whilst at $-20^\circ C$, the best energy resolution was $770 eV$ using a shaping time of $10 \mu s$. System noise analysis was also carried out. The different noise contributions were computed as a function of temperature. The main source of noise limiting the energy resolution of the reported system was the dielectric noise. The dielectric noise contribution was found to increase as the temperature was increased.

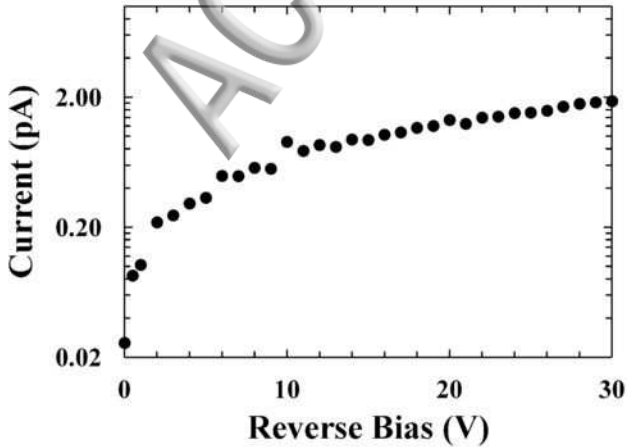
ACKNOWLEDGMENTS

This work was supported by STFC grants ST/M002772/1 and ST/M004635/1 (University of Sussex, A. M. B., PI) and Royal Society Grant RS130515 (University of Sussex, A. M. B., PI). The authors are grateful to R. J. Airey and S. Kumar at the EPSRC National Centre for III-V Technologies for device fabrication. G. Lioliou acknowledges funding received in the form of a PhD scholarship from the University of Sussex. T. Gohil acknowledges funding received in the form of a PhD studentship from the Engineering and Physical Sciences Research Council, UK, and the University of Sussex, UK.

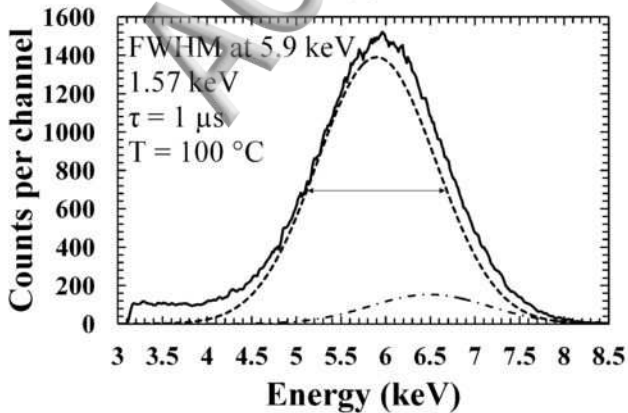
REFERENCES

- ¹ S. Butera, G. Lioliou, A. B. Krysa, and A. M. Barnett, J. Appl. Phys. 120, 024502 (2016).
- ² A. Auckloo, J. S. Cheong, X. Meng, C. H. Tan, J. S. Ng, A. B. Krysa, R. C. Tozer, and J. P. R. David, J. Inst. 11, P03021 (2016).
- ³ J. S. Cheong, J. S. Ong, J. S. Ng, A. B. Krysa, and J. P. R. David, IEEE J. Sel. Topics Quantum Electron. 20, 142 (2014).
- ⁴ J. S. L. Ong, J. S. Ng, A. B. Krysa, and J. P. R. David, IEEE Electron Device Letters 32, 1528 (2011).
- ⁵ L. Qiao, J. S. Cheong, J. S. Ong, J. S. Ng, A. B. Krysa, A. B. Green and J. P. R. David, IEEE Photon. Technol. Lett. 28, 481 (2016).
- ⁶ D. T. Cromer, and D. Liberman, J. Chem. Phys 53, 1891 (1970).
- ⁷ R. Jenkins, R. W. Gould, and D. Gedcke, *Quantitative X-ray Spectrometry*, Second Ed. (CRC Press, New York, 1995).
- ⁸ U. V. Desnica, Prog. Cryst. Growth Charact. Mater. 36, 291 (1998).
- ⁹ G. Bertuccio, S. Caccia, D. Puglisi, and D. Macera, Nucl. Instrum. Meth. Phys. Res., Sect. A 652, 193 (2011).
- ¹⁰ A. M. Barnett, D. J. Bassford, J. E. Lees, J. S. Ng, C. H. Tan, and J. P. R. David, Nucl. Instrum. Meth. Phys. Res., Sect. A 621, 453 (2010).
- ¹¹ A. M. Barnett, J. E. Lees, D. J. Bassford, J. S. Ng, C. H. Tan, N. Babazadeh, and R. B. Gomes, Nucl. Instrum. Meth. Phys. Res., Sect. A 654, 336 (2011).
- ¹² G. Lioliou, X. Meng, J. S. Ng, and A. M. Barnett, J. Appl. Phys. 119, 124507 (2016).
- ¹³ A. Owens, *Compound semiconductor radiation detectors*, (CRC Press, Boca Raton, 2012).
- ¹⁴ M. R. Squillante and G. Entine Nucl. Instrum. Meth. Phys. Res. A 380, 160 (1996).
- ¹⁵ S. U. Egarievwe, K. T. Chen, A. Burger, R. B. James, and C.M. Lisse, J. X-ray Sci. Technol. 6, 309 (1996).
- ¹⁶ P. J. Sellin, Nucl. Instr. and Meth. A 563, 1 (2006).
- ¹⁷ M. D. Wilson, S. J. Bell, R. J. Cernik, C. Christodoulou, C. K. Egan, D. O'Flynn, S. Jacques, S. Pani, J. Scuffham, P. Seller, P. J. Sellin, R. Speller, and M. C. Veale, IEEE Trans. Nucl. Sci. 60, 1197 (2013).

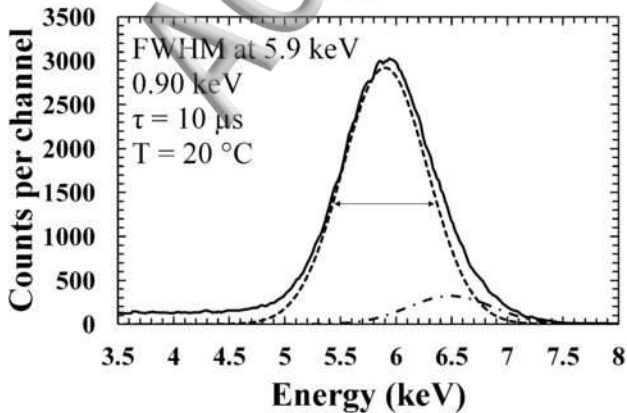
- ¹⁸ L. Abbene, G. Gerardi, and F. Principato, *Nucl. Instrum. Meth. Phys. Res. A* **777**, 54 (2015).
- ¹⁹ M. Prokesch, S. A. Soldner, A. G. Sundaram, M. D. Reed, H. Li, J. F. Eger, J. L. Reiber, C. L. Shanor, C. L. Wray, A. J. Emerick, A. F. Peters, and C. L. Jones, *IEEE Trans. Nucl. Sci.* **63**, 1854 (2016).
- ²⁰ L. Abbene, G. Gerardi, A. A. Turturici, G. Raso, G. Benassi, M. Bettelli, N. Zambelli, A. Zappettini, and F. Principato, *Nucl. Instrum. Meth. Phys. Res. A* **835**, 1 (2016).
- ²¹ A. Zappettini, D. Macera, G. Benassi, N. Zambelli, D. Calestani, M. Ahangarianabhari, Y. Shi, G. Rotondo, B. Garavelli, P. Pozzi, and G. Bertuccio, *IEEE Nuclear Science Symposium and Medical Imaging Conference (NSS/MIC)*, (2014).
- ²² Keithley Instruments, Inc, *Model 6487 Multi-Frequency LCR Meter Manual*, 6487-901-01 Rev B, (Cleveland, 2011).
- ²³ Bertuccio, P. Rehak, and D. Xi, *Nucl. Instrum. Meth. Phys. Res. B* **326**, 71 (1993).
- ²⁴ U. Shotzig, *Applied Radiation and Isotopes* **53**, 469 (2000).
- ²⁵ G. Lioliou, and A. M. Barnett, *Nucl. Instrum. Meth. Phys. Res. A* **801**, 63 (2015).
- ²⁶ S. Butera, G. Lioliou, A. B. Krysa, and A. M. Barnett, *Electron-hole pair creation energy in Al_{0.52}In_{0.48}P*, submitted to *Sci. Rep.* (2016).
- ²⁷ G. A. Bertuccio, A. Pullia, and G. De Geronimo, *Nucl. Instrum. Meth. Phys. Res. A* **380**, 301 (1996).
- ²⁸ E. Gatti, P. F. Manfredi, M. Sampietro, and V. Speziali, *Nucl. Instrum. Meth. Phys. Res., A* **297**, 467 (1990).
- ²⁹ G. Bertuccio, and D. Maiocchi, *J. Appl. Phys.* **92**, 1248 (2002).



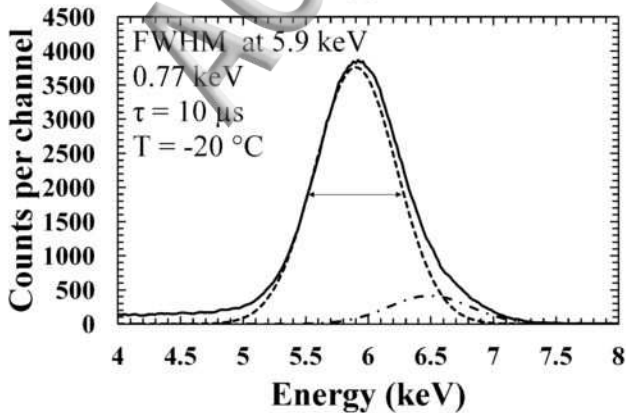
(a)

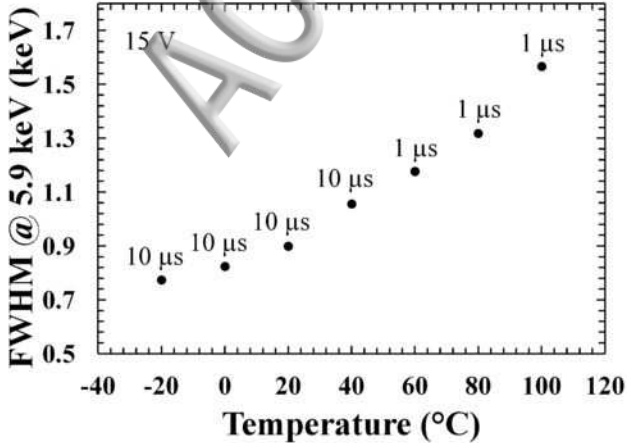


(b)



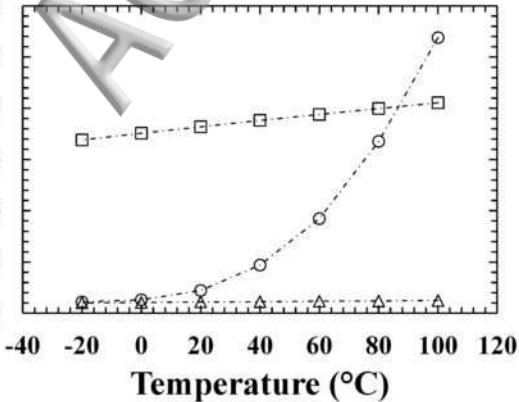
(c)





Computed Equivalent
Noise Charge (e^- rms)

60
50
40
30
20
10
0



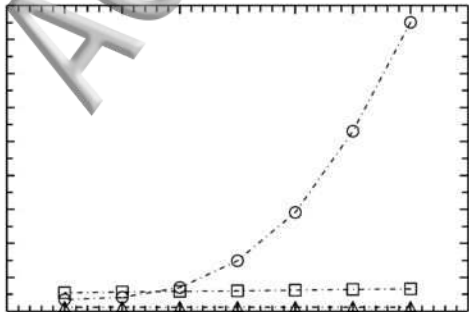
Computed Equivalent
Noise Charge (e^- rms)

180
160
140
120
100
80
60
40
20
0

-40 -20 0 20 40 60 80 100 120

Temperature ($^{\circ}\text{C}$)

(b)



Equivalent Noise Charge

(e^- rms)

